Antarctic Science 7 (4): 421–433 (1995)

A case study of turbulent parameters during the Antarctic winter

CARLOS YAGÜE[1] and JOSÉ M. REDONDO[2]

[1]Departamento de Física de la Tierra, Astronomía y Astrofísica II. Facultad de Ciencias Físicas, Universidad Complutense de Madrid, 28040 Madrid, Spain

[2]Departament de Física Aplicada, Jordi Girona 31, Universitat Politécnica de Catalunya, 08034 Barcelona, Spain

Abstract: Two days of the Antarctic winter (20 and 21 June 1986) were chosen to study some turbulent parameters in this particular boundary-layer. Richardson number, Monin-Obukhov length, eddy transfer coefficients, turbulent kinetic energy, turbulent intensities, friction velocities and sensible heat flux at three levels (5, 17 and 32 m) were considered. The results show how the stability at 17 and 32 m influences the turbulent transfer at 5 m. The shear of wind is the main mechanism to produce mixing in the lower atmosphere at Antarctica, and thermal inversions associated to surface cooling develop with winds < 10 m s^{-1} at 5 m. The possible influence of internal gravity-waves on the atmospheric boundary-layer during strong stable stratification is studied.

Received 30 March 1995, accepted 30 June 1995

Key words: stable boundary-layer, turbulent exchange, surface thermal inversions

Introduction

The winter lower atmosphere at the Halley Research Station (Antarctica) is especially useful for the study of boundary-layer problems due to the following characteristics: absence of the diurnal solar heating, homogeneity of the ice sheet where the observatory is located and the presence of strong thermal inversions which are rarely observed in other latitudes. The importance of the processes taking place in the nocturnal boundary-layer has been reported by several authors (Kondo *et al.* 1978, Nieuwstadt 1984, Hunt *et al.* 1985). There are also a few recent papers investigating the boundary-layer in the Arctic (Walter & Overland 1991, Bradley *et al.* 1993) and Antarctic sites (King 1990, Pasricha *et al.* 1991, Rees 1991, Egger *et al.* 1993, King & Anderson 1994, Yagüe & Cano 1994) when the stable boundary-layer can be analysed in detail due to these circumstances.

King (1993) pointed out the main differences between the Antarctic stable boundary-layer and the nocturnal boundary-layer observed at mid-latitude observatories:

a) the significant stable stratification in the lower troposphere,

b) the slope-induced baroclinity and

c) the gravity-wave effects.

The role of internal gravity-waves and their connection to turbulence, is one the key factors in the understanding of the stable boundary-layer (Einaudi & Finnigan 1993). At Halley there seem to be several mechanisms for the generation of internal gravity-waves, such as: topographic forcing due to undulations in the ice shelf (Rees & Mobbs 1988), locally generated instabilities or turbulence (Mobbs & Rees 1989) and waves created by dynamical instabilities in shear layers above the surface (Rees 1987).

In this paper several turbulent parameters have been studied on two days (20 and 21 June 1986). An evolution from near-neutral to strong stable stratification is observed during this period and analysed in detail. The stratification has been parameterized by means of the gradient Richardson number (Ri) and the Monin-Obukhov length (L). Friction velocity (u_*) and the eddy transfer of heat (K_h) and momentum (K_m) have been evaluated in order to study the turbulence. The influence of internal gravity-waves has been investigated from measurements of turbulence intensities and the strength of surface inversions, which are usually present at Halley.

Meteorological data

The British Antarctic Survey ran the project STABLE (Stable Antarctic Boundary-layer Experiment) during the winter of 1986 at Halley Research Station, which is situated near the seaward edge of the Brunt Ice Shelf (76.6°S, 26.7°W). It can be considered as homogeneous and flat terrain and King (1990) found a roughness length of the order of 10^{-4} m. The data were obtained from a 32 m meteorological mast supporting three sonic thermo-anemometers (Kaijo-Denki model Dat-100) at 5, 17 and 32 m, and platinum resistance thermometers (Vector Instruments T302) which were used to measure temperature differences between 2–4, 4–8, 8–16 and 16–32 m. Additionally three cup anemometers (Vector Instruments A100) were deployed at 2, 8 and 24 m, although their measurements have to be used with care as for slow winds riming may damp the response of these anemometers. King & Anderson (1988) made intercomparisons between the cup and sonic anemometers, and showed that for wind speeds <5 m s^{-1} there was poor agreement between the readings due to the ice build-up. On the other hand for wind speeds >5 m s^{-1} the cup anemometer reads about 5% above the speed measured by the ultrasonic anemometer, so cup anemometer

https://doi.org/10.1017/S0954102095000587 Published online by Cambridge University Press

data have been considered only for wind speeds >5 m s^{-1} and have been multiplied by 0.95. Data with winds at 5 m less than 2 m s^{-1} or greater than 11 m s^{-1} have been excluded. The former restriction is due to significant errors appearing in ultrasonic readings for such low velocities as a result of ice build-up. The latter is because at higher velocities drifting snow may cause the aerodynamic characteristics of the snow surface to vary quickly. Change of wind direction with height has also been taken into account, so when the difference in wind direction between 5 and 32 m (where direction is measured) is >20° the data have not been considered in order to fit a wind profile and neither Ri nor K_m have been evaluated and they are not shown in the plots. In the remaining cases it is supposed that there exists a constant (or nearly) wind direction with height (Haltiner & Martin 1957, p.227).

The ultrasonic thermo-anemometer at 5 m supplies the absolute temperature at this level. In order to obtain the temperatures at 2, 4, 8, 16 and 32 m a linear temperature gradient was assumed between 4–8 m. From the 5 m reference temperature, the temperature difference measurement could then be used to infer the temperature at any other level. Absolute temperatures can be converted to potential temperatures using the relationship $(\partial\theta/\partial z) \simeq (\partial T/\partial z) + 0.0098$ or $\Delta\theta \simeq \Delta T + 0.0098\Delta Z$ (Arya 1988, p.172). The resistance thermometers and the cup anemometer data were sampled at 1 Hz and the ultrasonic thermo-anemometer data at 5 Hz. All the variables as well as the covariances and variances of velocity ($\overline{u'w'}$, $\overline{v'w'}$, $\overline{u'v'}$, $\overline{u'^2}$, $\overline{v'^2}$, $\overline{w'^2}$) and temperature ($\overline{\theta'w'}$,$\overline{\theta'^2}$) were averaged over 10 min. In the present work 1 h average of the 10 min data have been used. Further information about the STABLE project and the corrections to the data can be found in (King & Anderson 1988, King 1990). The two days analysed in this study (20 and 21 June 1986) have been chosen because they represent quite well the evolutions of turbulent parameters that can be found in Antarctica and also because of the total absence of diurnal effects, as these were days of total darkness. For practical reasons the data are presented divided in two days, but the events reflected in the evolution plots are, naturally, independent of the diurnal cycle.

Methodology

In this paper we have used a local scaling hypothesis to evaluate the turbulent parameters. This can be done in situations where turbulence aloft is disconnected with the surface (Wyngaard 1973, Nieuwstadt 1984). The stable boundary-layer can be quite shallow in the Antarctic winter, so at relatively short distance from the ground the turbulence may not be in equilibrium with surface fluxes and hence local fluxes, shears and stability are more important than surface values. The relevant height and velocity scales (which will be defined later) in this case (Stull 1988, p. 358) are of the

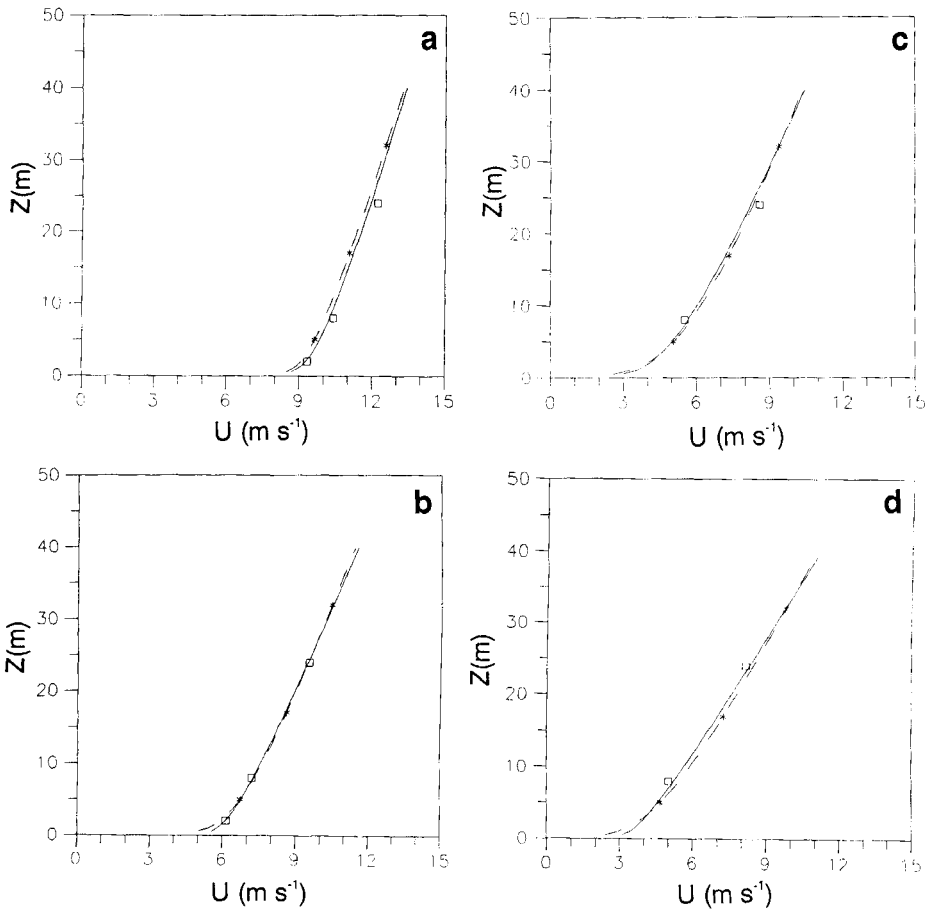


Fig. 1. Wind measurements from the sonic (*) and cup (□) anemometers (whenever $\bar{u}$ >5 m s^{-1}). The solid line represents the log-linear fit to the cup and sonic readings and the dashed line only to the sonic measurements. **a.** 20 June 0700h, **b.** 20 June 14h00, **c.** 21 June 03h00, **d.** 21 June 12h00.

https://doi.org/10.1017/S0954102095000587 Published online by Cambridge University Press

order of 0–50 m (L, local Monin-Obukhov height) and 0–0.3 m s^{-1} (u_*, local friction velocity), respectively. In a stable boundary-layer the vertical size of a turbulent eddy is restricted, so that turbulence cannot feel the presence of the surface. As a result, the boundary-layer structure no longer depends explicitly onz. This is called the z-less stratification (Wyngaard 1973). The consequence of z-less stratification for local scaling is the important result that dimensionless quantities approach a constant value in the limit $z/L \rightarrow \infty$. Although dimensionless groups formed with these scales are not a function of height above ground (z-less scaling), the individual variables that make up these groups (including L and u_*) change significantly with height.

Log-linear profiles were fitted to the mean wind speed ($\overline{u}$) and temperature ($\overline{T}$) using least-squares procedure in a similar way as Nieuwstadt (1984) and King (1990):

$$\overline{u} = a + b \ln(z) + c\,z \tag{1}$$

$$\overline{T} = a' + b' \ln(z) + c'\,z \tag{2}$$

An interesting point is to compare the wind profiles fitted only to the sonic readings (5, 17 and 32 m), and those obtained using both, sonic and cup anemometers (whenever possible, $\overline{u} > 5$ m s^{-1}) data. It is important to get a good fit of the wind profile as $\partial\overline{u}/\partial z$ is evaluated from this profile and the values of Richardson number and the eddy transfer coefficient for momentum depend on $\partial\overline{u}/\partial z$ as will be next shown. Fig. 1 (a–d) shows, for four specific hours (with different wind regimes), the wind measurements at all available levels, the log-linear fit (1) using only the sonic readings (dashed line), and the fit including the cup anemometers (solid line). Both log-linear curves fit the readings quite well (with correlation coefficients >0.99), so similar results are expected whether or not cup anemometers are included. However, this point will be analysed later.

Another remarkable feature of the wind readings is related to the fact that the cup anemometers seem to read progressively less than the sonics (see Fig. 1c comparing cup anemometer readings at 8 and 24 m). Some reasons for this result could be: a) slight rime accumulation, b) non-linearity in wind speed response as the wind drops, c)systematic error in the cup anemometers as the stability increases and the associated turbulence is suppresed. It is difficult to established which one is the most important reason. However, it is logical to think that the above causes are connected. The increasing stability favours rime accumulation and the low winds, which would, in turn lead to errors in the wind speed. So the low winds (measured by cup anemometers) are probably more affected by errors and these winds are present at heights closer to the ground (as the wind speed increases with height).

Temperature profiles have been fitted to six levels (2, 4, 5, 8, 16 and 32 m).

Once these fits have been made, the gradient Richardson number can be calculated in a straight-forward manner:

$$Ri = \frac{(g/\theta_0)\dfrac{\partial\overline{\theta}}{\partial z}}{\left(\dfrac{\partial\overline{u}}{\partial z}\right)^2} \tag{3}$$

The friction velocity (u_*) and Monin-Obukhov length (L) are defined as:

$$u_* = \left[\overline{(u'w')}^2 + \overline{(v'w')}^2\right]^{1/4} \tag{4}$$

$$L = -\frac{u_*^3 T_0}{k g \overline{w'\theta'}} \tag{5}$$

where k is the von Kármán constant (0.41), g the acceleration due to gravity and T_0 reference temperatures.

The turbulence intensity has been evaluated (at different levels) for each component as (Arya 1988, p.118):

$$i_u = \frac{\overline{(u'^2)}^{1/2}}{\overline{u}} \tag{6}$$

$$i_v = \frac{\overline{(v'^2)}^{1/2}}{\overline{u}} \tag{7}$$

$$i_w = \frac{\overline{(w'^2)}^{1/2}}{\overline{u}} \tag{8}$$

where $\overline{u}$ is the wind speed.

The eddy transfer coefficients for momentum and heat and the sensible heat flux are respectively:

$$K_m = \frac{\overline{-u'w'}}{\dfrac{\partial\overline{u}}{\partial z}} \tag{9}$$

$$K_h = \frac{-\overline{\theta'w'}}{\dfrac{\partial\overline{\theta}}{\partial z}} \tag{10}$$

$$H = \rho\, C_p\, \overline{w'\theta'} \tag{11}$$

The temporal evolution of all these parameters has been evaluated. Another important parameter in the description of the flow is the turbulent kinetic energy, defined as:

$$\mathrm{TKE} = \frac{1}{2}\left(\overline{u'^2} + \overline{v'^2} + \overline{w'^2}\right) \tag{12}$$

Finally, the influence of the surface inversions, whose strength has been parameterized by $(\Delta T)_{32-2}$ (temperature difference

https://doi.org/10.1017/S0954102095000587 Published online by Cambridge University Press

between 32 and 2 m), on turbulence characteristics has been investigated.

Results

First we consider the differences obtained in Ri and K_m (for the three levels studied) according to whether $\bar{u}$ is evaluated from the fit to the sonic anemometers readings (fit A) or both sonic and cup anemometers (with $\bar{u} > 5$ m s^{-1}) data (fit B). In Fig. 2 the values of Richardson number obtained with fits A and B can be compared, for 20 and 21 June and for the three levels studied (5, 17 and 32 m), The differences are especially small at 17 m. At 5 m the values with fit A are smaller than for fit B and the opposite at 32 m. This arises because, as can be seen in Fig. 1 (except for Fig. 1a where both fits have practically the same slope, giving the same Ri from fit A or B for the three heights) the slope is slightly higher at 5 m for fit A than for fit B producing smaller values of Ri at 5 m, and the opposite happens at 32 m. However, the evolution of Ri is similar for both fits. If K_m is now compared (Fig. 3), the differences between fits A and B are smaller than for Richardson number and K_m also has the same evolution whether fit A or B is used.

Since it has been shown that no essential differences are

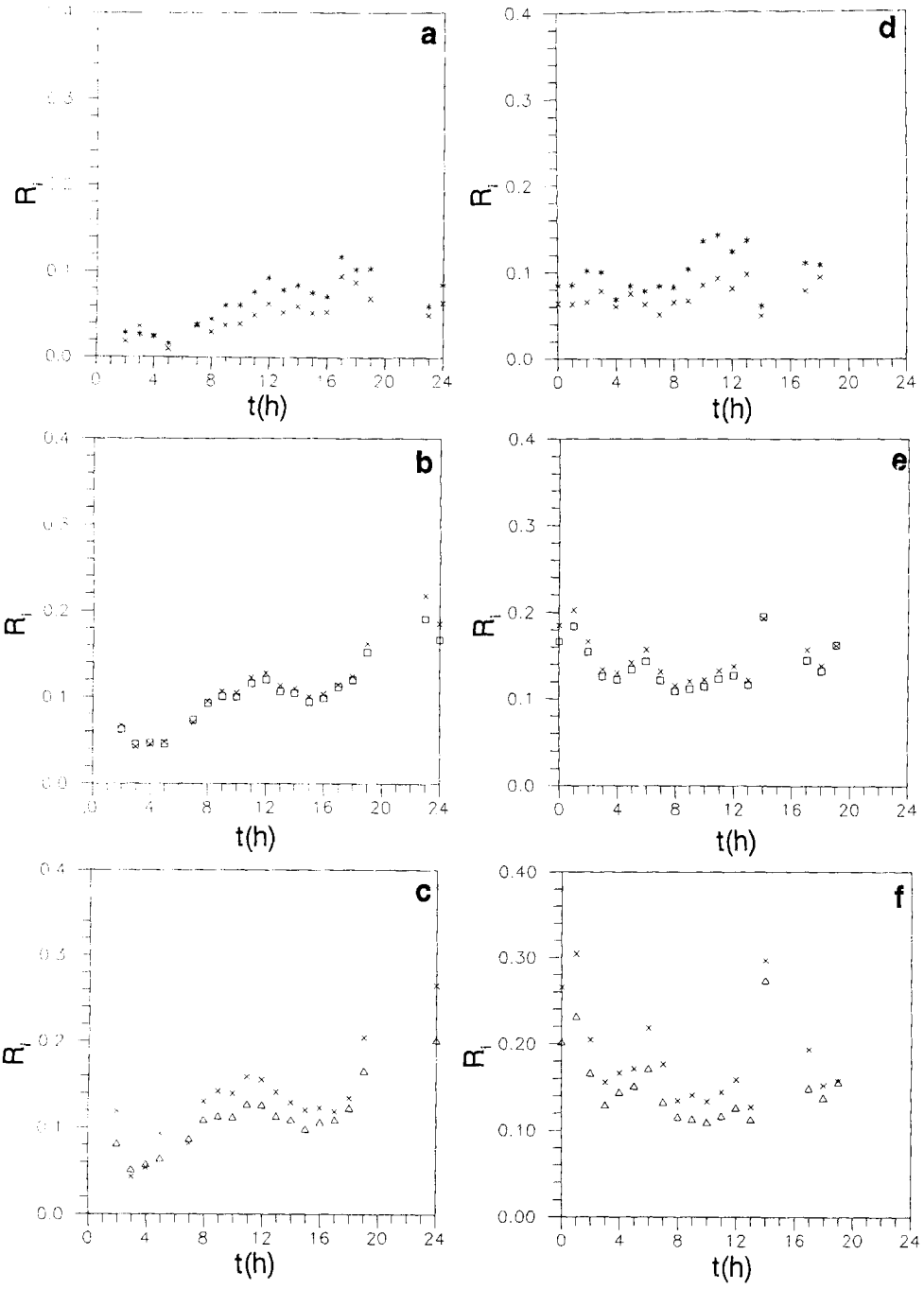


Fig. 2. Comparison of Ri evaluated using the wind speed fit to the sonic readings or the fit to the cup and sonic readings for 20 June: **a.** 5 m (*), **b.** 17 m. (□), **c.** 32 m (Δ), and 21 June: **d.** 5 m (*), **e.** 17 m. (□), **f.** 32 m (Δ). The symbol x is used for the three levels when Ri is calculated from the fit to the sonic readings.

https://doi.org/10.1017/S0954102095000587 Published online by Cambridge University Press

obtained in Ri and K_m depending on which fit is chosen, the second one (B) will be used.

Observations for 20 and 21 June 1986 will be first analysed separately and later, factors common to both days will be discussed. The temporal evolutions of the eddy transfer coefficients (K_m and K_h) for 20 June are shown in Fig. 4a & b respectively. Three periods can be distinguished (mean values of the main turbulent paramenters are summarized in Table I for these periods): the first one would be from 0–7h, with high values of turbulent transfer coefficients. K_m and K_h have been calculated at three heights : 5 m (*), 17 m (□) and 32 m (Δ). The largest differences between the three heights are seen in this period; the highest values appear at the 32 m level indicating that eddy transfer coefficients increase with height. There is no solar forcing (in the two days analysed) and the wind shear seems to be the main source producing turbulence. This agrees well with the behaviour of friction velocity (Fig. 4c); this period of time (0–7h) has the highest values of u_* but differences with height are not significant indicating a constant momentum flux layer. On the other hand similar friction velocities at different levels produce different K_m and K_h, giving larger turbulent transfer coefficients further from the ground, which is in good agreement with other estimations of the vertical variations of turbulent transfer

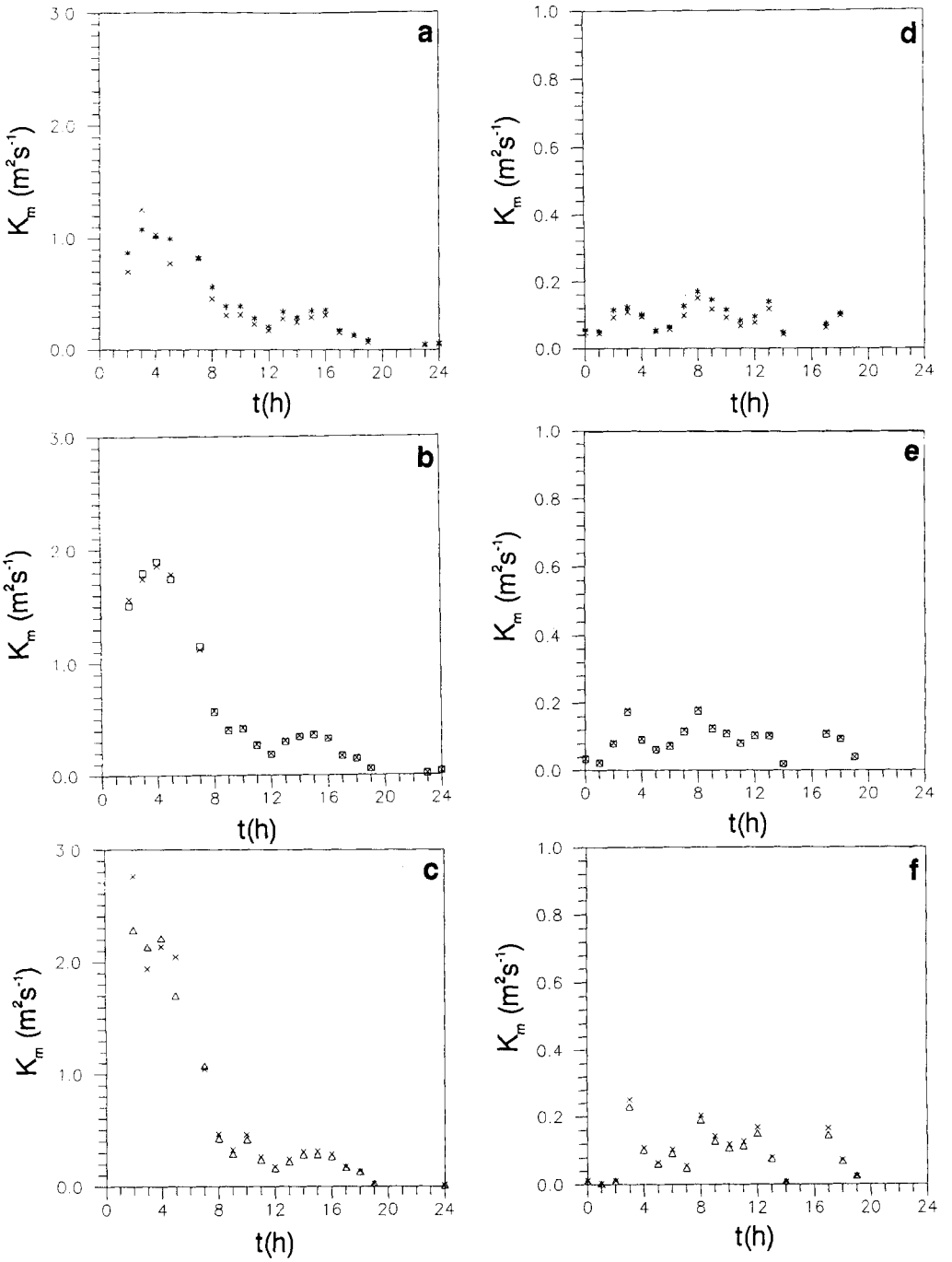


Fig. 3. Comparison of K_m evaluated using the wind speed fit to the sonic readings or the fit to the cup and sonic readings for 20 June: **a.** 5 m (*), **b.** 17 m. (□), **c.** 32 m (Δ), and 21 June: **d.** 5 m (*), **e.** 17 m. (□), **f.** 32 m (Δ). The symbol x is used for the three levels when K_m is calculated from the fit to the sonic readings.

https://doi.org/10.1017/S0954102095000587 Published online by Cambridge University Press

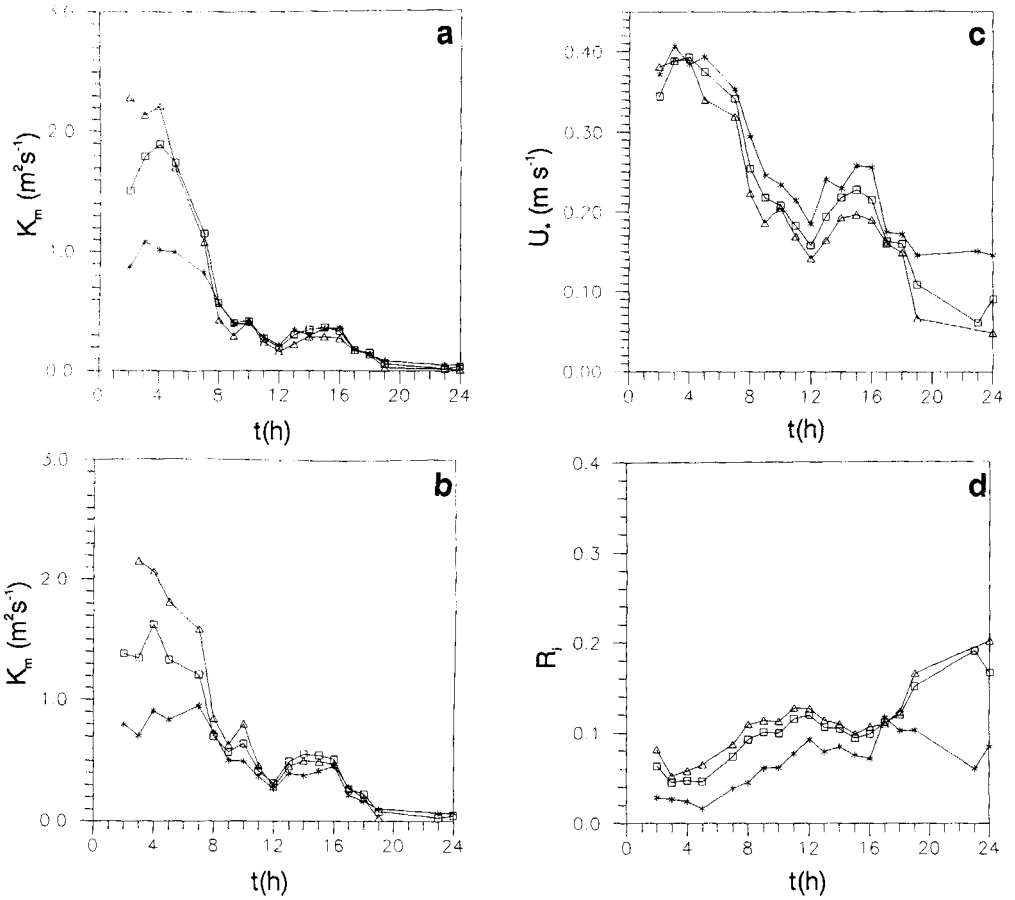


Fig. 4. **a.** Eddy transfer coefficient for momentum K_m, **b.** eddy transfer coefficient for heat K_h, **c.** friction velocity u_*, **d.** Richardson number Ri for 20 June . The meaning of symbols are: (*) 5m, (□) 17m, (Δ) 32m.

Table I. Mean values of turbulent parameters for the three periods established on 20 June.

Time	Height(m)	Ri	K_m(m^2s^{-1})	K_h(m^2s^{-1})	L(m)	u(m s^{-1})	u_*(m s^{-1})
00h00–07h00	5	0.027	0.95	0.84	292.4	10.2	0.38
	17	0.055	1.61	1.40	248.5	11.5	0.37
	32	0.069	1.88	1.86	205.6	12.7	0.36
08h00–18h00	5	0.078	0.32	0.40	37.6	6.6	0.23
	17	0.106	0.32	0.47	25.2	8.4	0.20
	32	0.114	0.26	0.49	18.7	10.2	0.18
19h00–24h00	5	0.083	0.062	0.079	9.6	4.8	0.15
	17	0.17	0.035	0.051	4.3	8.1	0.09
	32	0.19	0.016	0.020	3.6	10.5	0.06

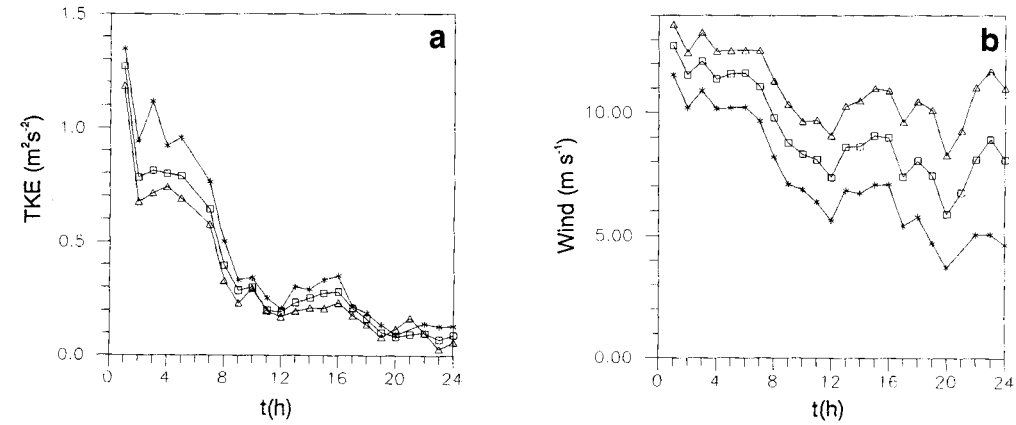


Fig. 5. **a.** Turbulent kinetic energy, **b.** wind speed for June 20. The symbols are as in Fig. 4.

https://doi.org/10.1017/S0954102095000587 Published online by Cambridge University Press

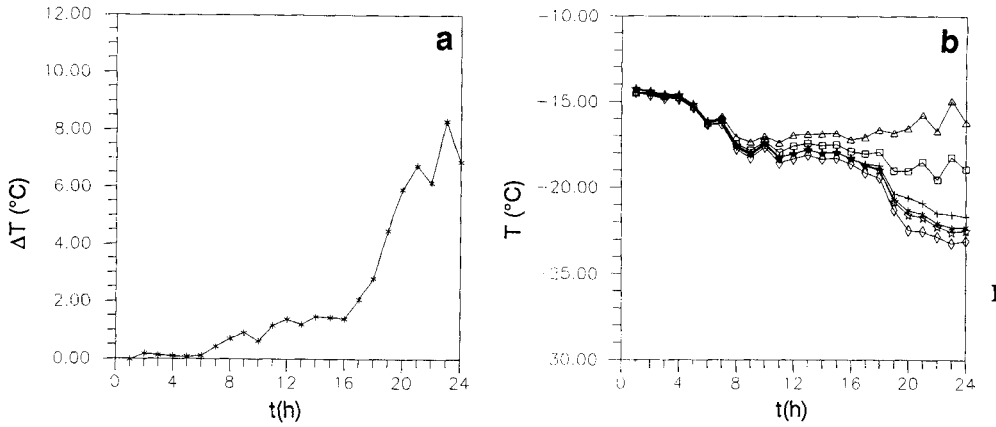


Fig. 6. **a.** Temperature difference between 32m and 2m, **b.** temperature at 2 m (◊), 4 m (★), 5 m (*), 8 m (+), 16 m (□) and 32 m (Δ) for 20 June.

coefficients (Brost & Wyngaard 1978, Wittich & Roth 1984) and with the relationship between K_m and u_* under near-neutral conditions ($K_m = kzu_*$). The gradient Richardson number, Ri (Fig. 4d) is < 0.05 at z=5 m and < 0.1 at 17 and 32 m, showing that stability is slight. The turbulent kinetic energy (TKE) is maximum (Fig. 5a), probably due to the strong winds at the three levels (>10 m s^{-1}), as can be observed in Fig. 5b. This wind regime does not allow the formation of a strong surface inversion as often happens in the Antarctic winter. This figure shows clearly a stronger vertical shear near the ground in the first period mentioned above (0–7h). The increment in temperature between 2 and 32 m is almost zero (Fig. 6a), due to the strong vertical mixing related to high TKE. The Monin-Obukhov length shows good agreement with the other stability parameter (Ri) and presents values > 150 m at the three levels (Fig. 7).

The second period corresponds roughly to the hours between 08h00 and 18h00. The eddy diffusivities of heat and momentum decrease as a consequence of the increasing stability (larger Richardson number and lower Monin-Obukhov length). The stability is clearly height dependent in this period and Ri is 0.1 at 17 and 32 m. The friction velocity decreases (on average) although a local maximum is reached *c.* 15h00 with the corresponding local maxima of K_m and K_h. Thermal inversion (Fig. 6a) is strengthening, especially from 16h00 to 18h00.

The final period for 20 June (19h00–24h00) is characterized by increasing stability with height, Ri > 0.15 at z=17, 32 m, and L<10 m for the three levels. The inversion strength reaches a maximum of 8°C and the eddy diffusivities of heat and momentum are quite close to zero, in good agreement with the low friction velocities obtained in this period. However, it is surprising that, in spite of the relatively strong winds at 32 m (~11 m s^{-1}), the eddy transfer coefficients are small. This can be explained by the strong stratification at Halley, which is not reached at mid-latitude observatories. King (1990) pointed out that background stability (up to 2000 m) in the Halley atmosphere could be responsible for this behaviour. He found, for example, as ϕ_m and ϕ_h (dimensionless forms of gradients of wind speed and potential temperature, respectively) did not have the same constants in

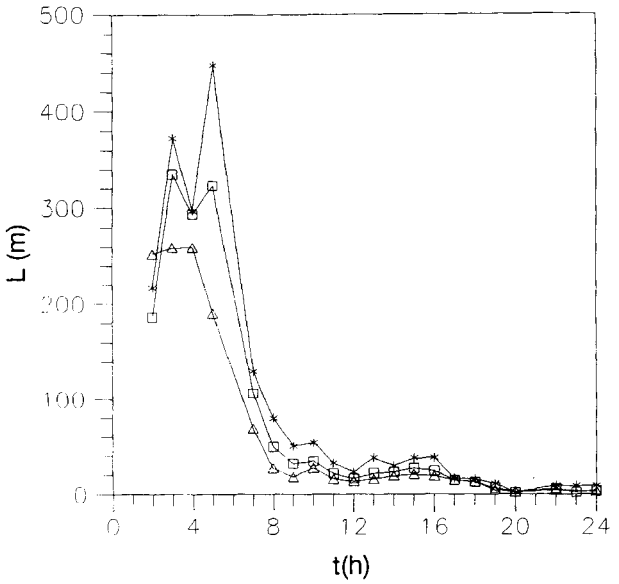


Fig. 7. Monin-Obukhov length for 20 June. The symbols are as in Fig. 4.

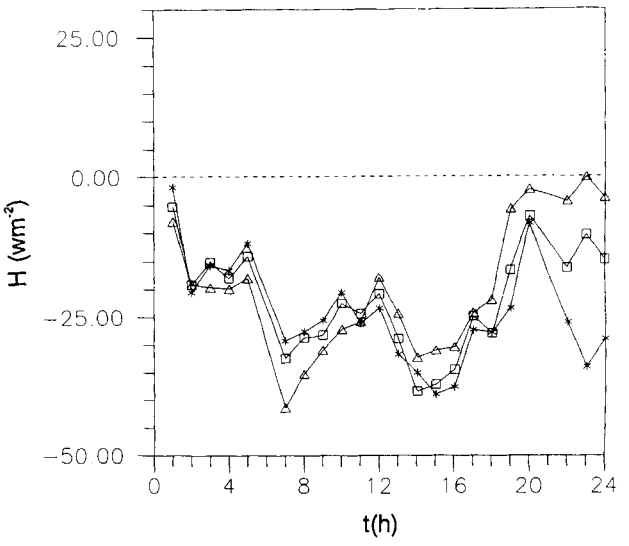


Fig. 8. Sensible heat flux for 20 June. The symbols are as in Fig. 4.

https://doi.org/10.1017/S0954102095000587 Published online by Cambridge University Press

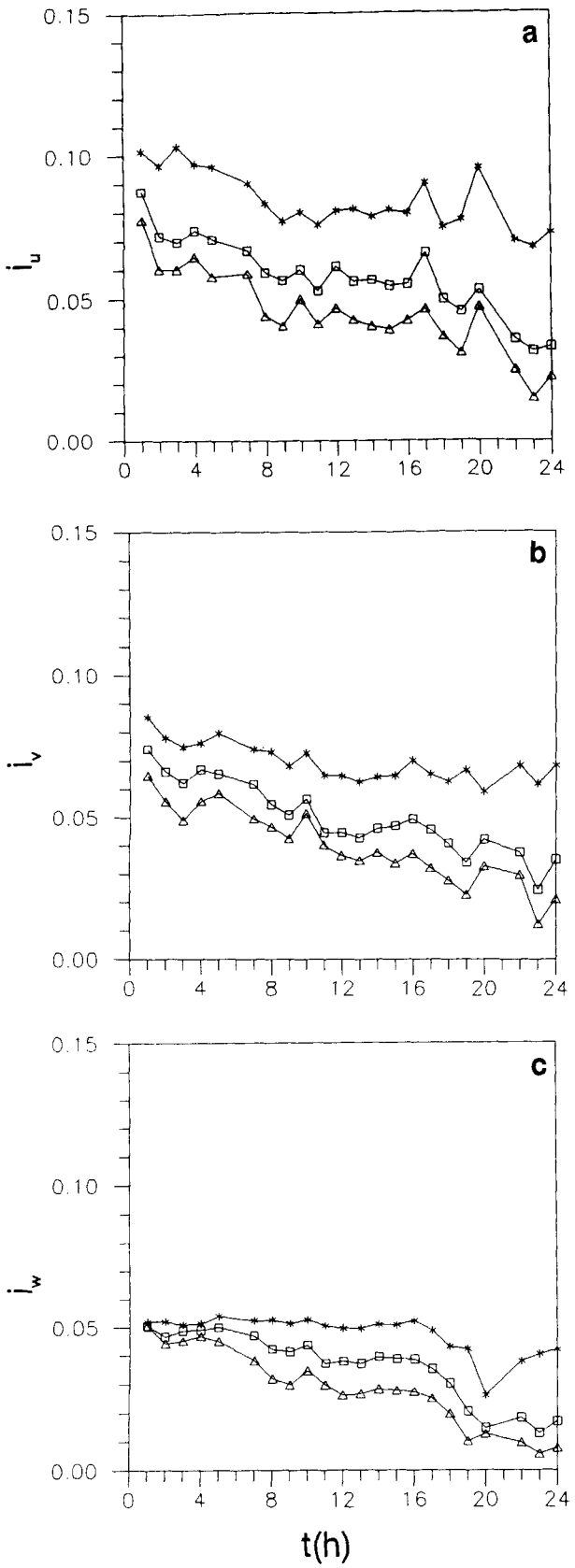


Fig. 9. Turbulence intensities for **a.** *u* component, **b.** *v* component, **c.** *w* component for 20 June . The symbols are as in Fig. 4.

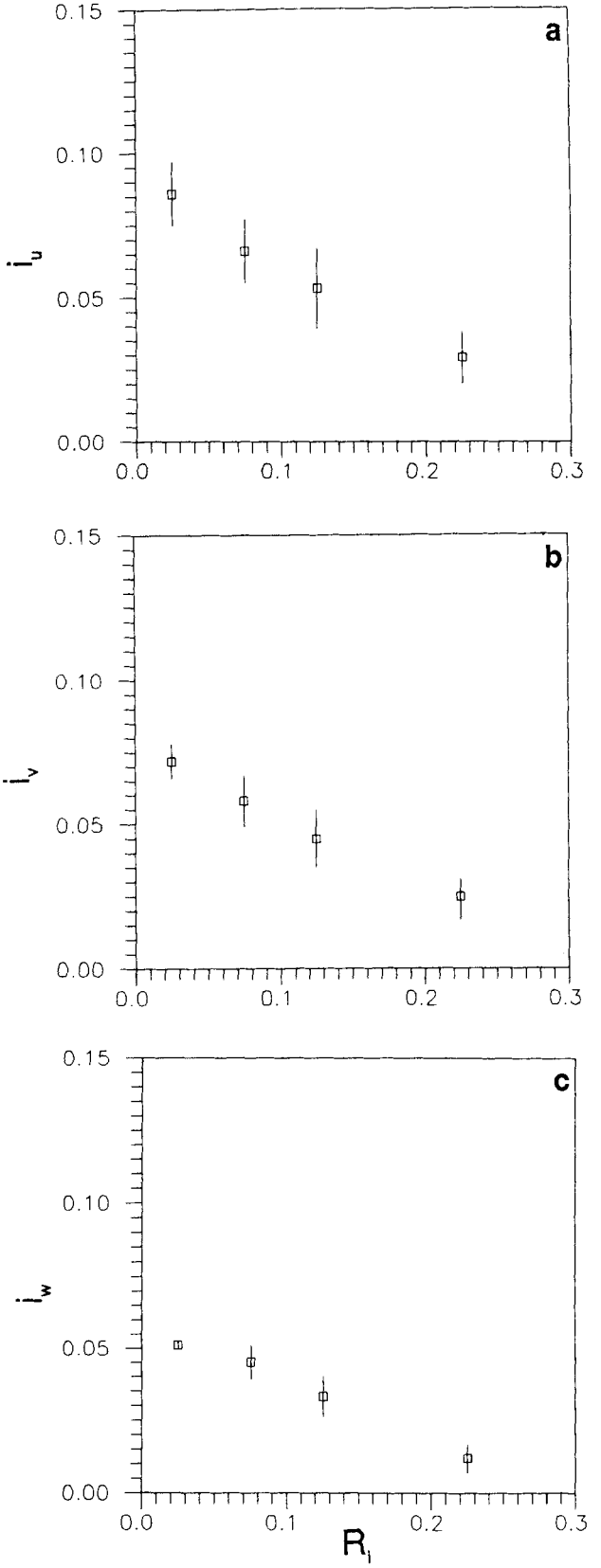


Fig. 10. Turbulence intensities versus Ri for **a.** u component, **b.** *v* component, **c.** *w* component for 20 June. The bars indicate the standard error.

https://doi.org/10.1017/S0954102095000587 Published online by Cambridge University Press

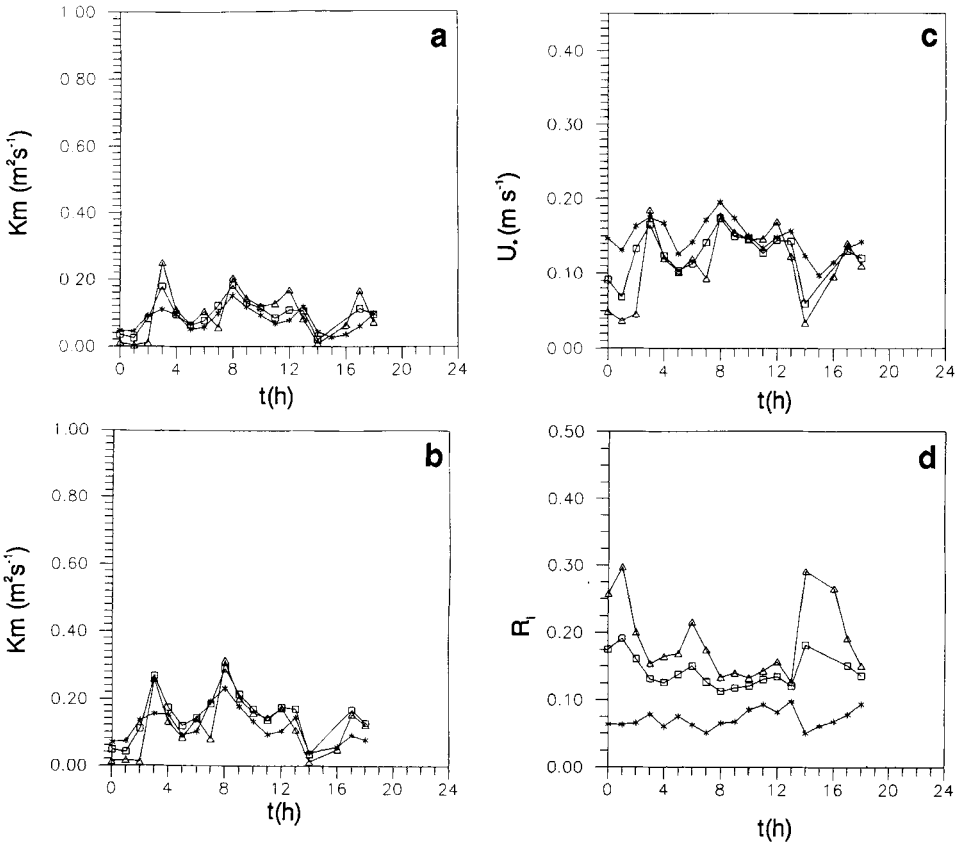


Fig. 11. **a.** Eddy transfer coefficient for momentum K_m, **b.** eddy transfer coefficient for heat K_h, **c.** friction velocity u_*, **d.** Richardson number Ri for 21 June. The symbols are as in Fig. 4.

the functional forms at different levels (≤32 m). This would mean that the surface-layer similarity theory can fail, even at such low heights.

Further explanations can be obtained if temporal evolution of temperature at six levels (2, 4, 5, 8, 16 and 32 m) is analysed (Fig. 6b). It is seen that the lower layers are cooling faster than the higher ones (especially 17 and 32 m), so the radiative cooling increases during this day, and the sensible heat flux directed toward the surface is not enough to balance the radiative cooling. The sensible heat flux (H) variations at 5, 17 and 32 m are shown in Fig. 8. These values are always negative (downward fluxes) and < 50 Wm^{-2}. The significant differences in height are especially important around the end of the day where an increase of stability and a strong decrease of H is observed with height. This lack of constancy in H would mean that the surface layer (where fluxes of momentum

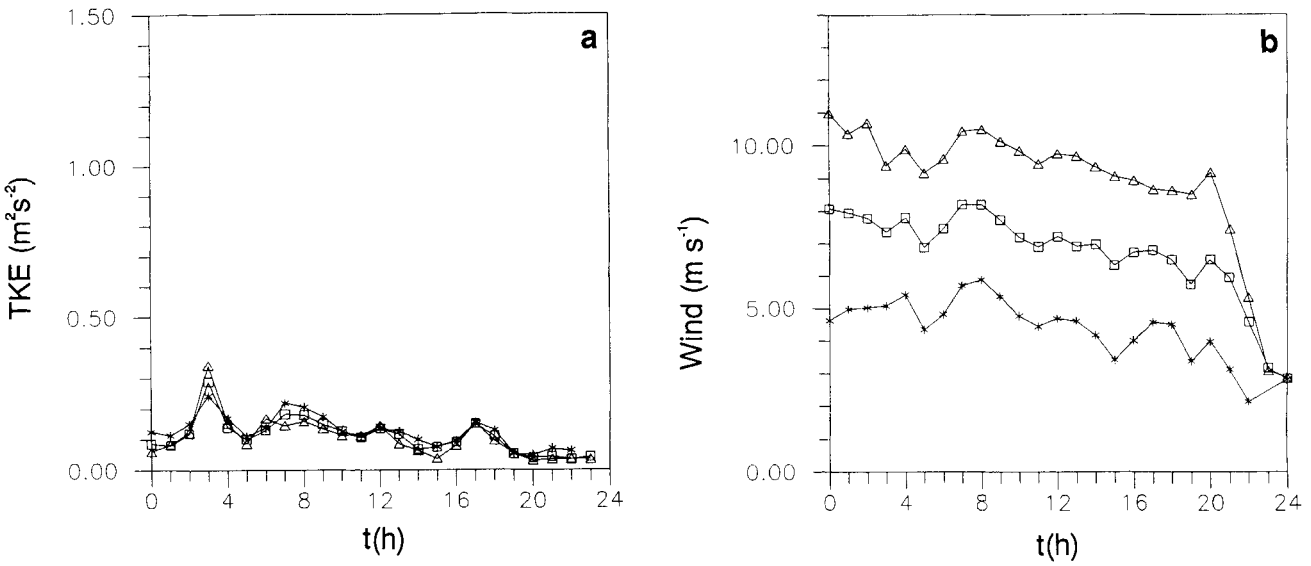


Fig. 12. **a.** Turbulent kinetic energy, **b.** wind for 21 June. The symbols are as in Fig.4.

https://doi.org/10.1017/S0954102095000587 Published online by Cambridge University Press

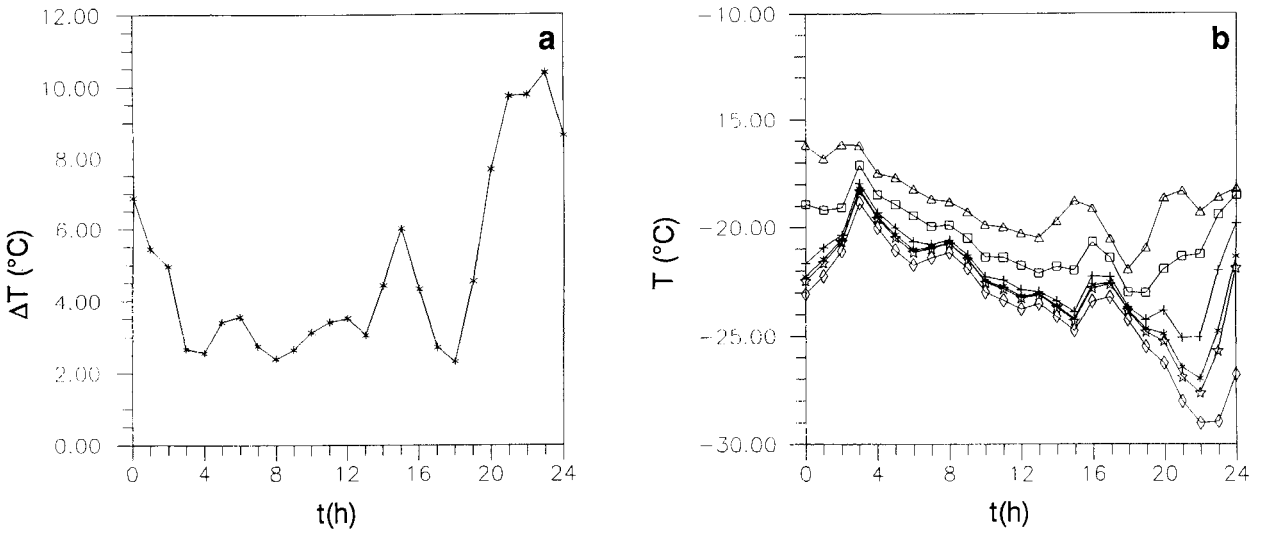


Fig. 13. **a.** Temperature difference between 32m and 2m, **b.** temperature at 2 m (◊), 4 m (★), 5 m (*), 8 m (+), 16 m (□) and 32 m (Δ) for 21 June.

and heat are roughly constant) is really shallow, *c.* 15 m if it is evaluated from $hf/u_* = 0.2$, for $u_* \simeq 0.1$ m s^{-1}; h is the boundary-layer height and the surface layer can be taken as the 10% of h closer to the ground (Arya 1988, p.2). This surface layer height can be even smaller if it is calculated as the height where H decreases a certain percentage (say 20%) of its surface value.

The turbulence intensities during 20 June are shown in Fig. 9a (i_u), 9b (i_v) and 9c (i_w) for the three levels analysed. The horizontal intensities (i_u and i_v) decrease with height, showing good agreement with the results obtained by Smedman (1991), who justifies this behaviour as a wall-effect (farther from the ground, more energy is transferred from the horizontal components to the vertical, for near neutral conditions). If i_w is analysed (Fig. 9c), from 01h00 to 05h00 there are no significant differences between the three levels, but as stability increases (from 06h00 onwards) the stratification acts as a sink of energy for the vertical component and this sink is greater as z increases due to the increasing stability with height (as seen before in Figs 4d & 7). This result is clearer if turbulence intensities are drawn versus Richardson number (see Fig. 10). Four intervals of Ri can be defined: (0–0.05), (0.05–0.1), (0.1–0.15) and (0.15–0.30); the mean values of turbulence intensities for each interval and the error bars (standard deviation) have been plotted. The decrease of i_u and i_v as Ri increases takes place throughout the Richardson number range, but for i_w the decrease is observed for sharper Ri when the stratification begins to produce a significant inhibition of vertical motions.

When 21 June is analysed in a similar way, several

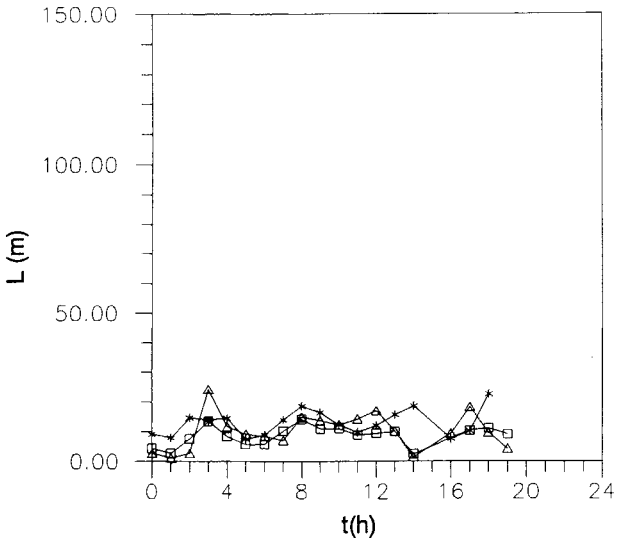


Fig. 14. Monin-Obukhov length for 21 June. The symbols are as in Fig. 4.

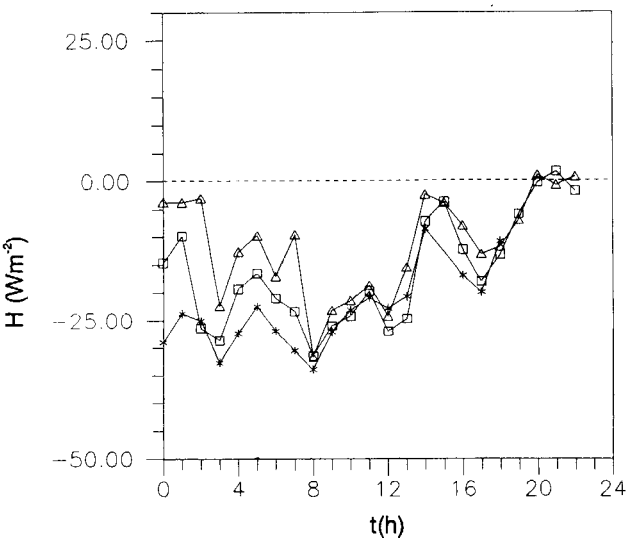


Fig. 15. Sensible heat flux for 21 June. The symbols are as in Fig. 4.

https://doi.org/10.1017/S0954102095000587 Published online by Cambridge University Press

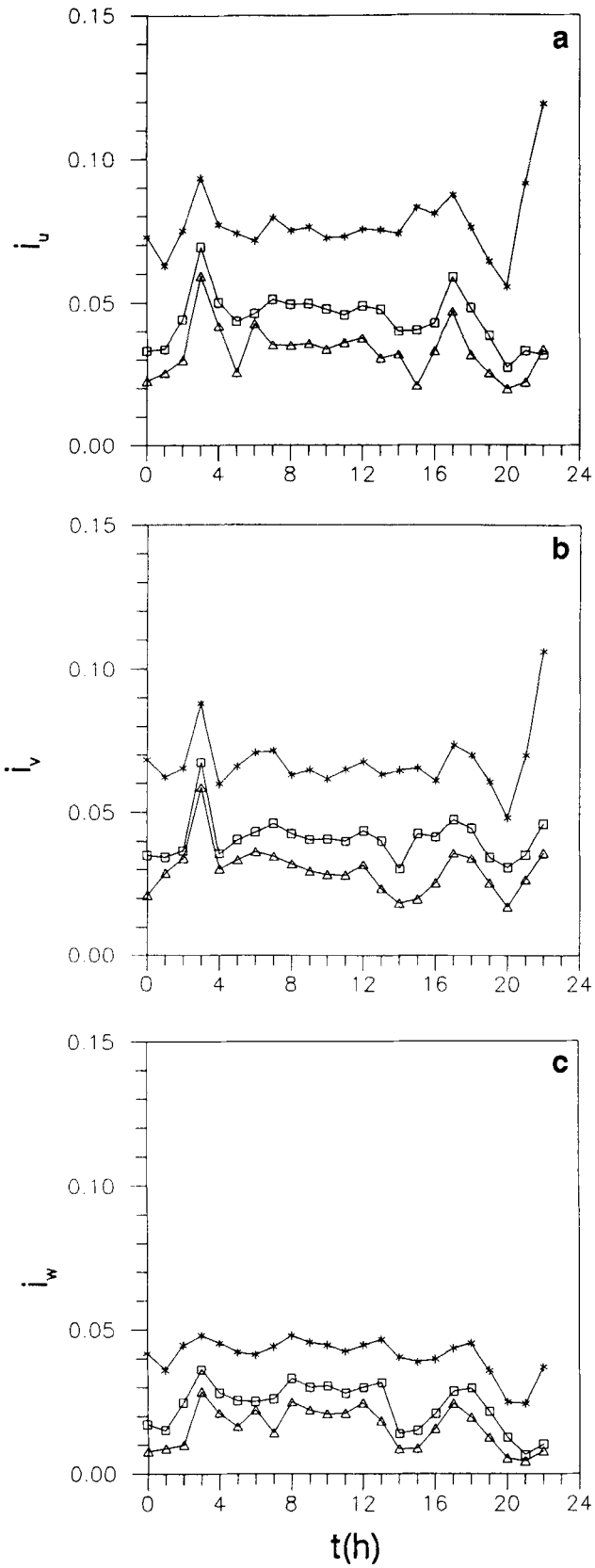


Fig. 16. Turbulence intensities for **a.** *u* component, **b.** *v* component, **c.** *w* component for 21 June . The symbols are as in Fig. 4.

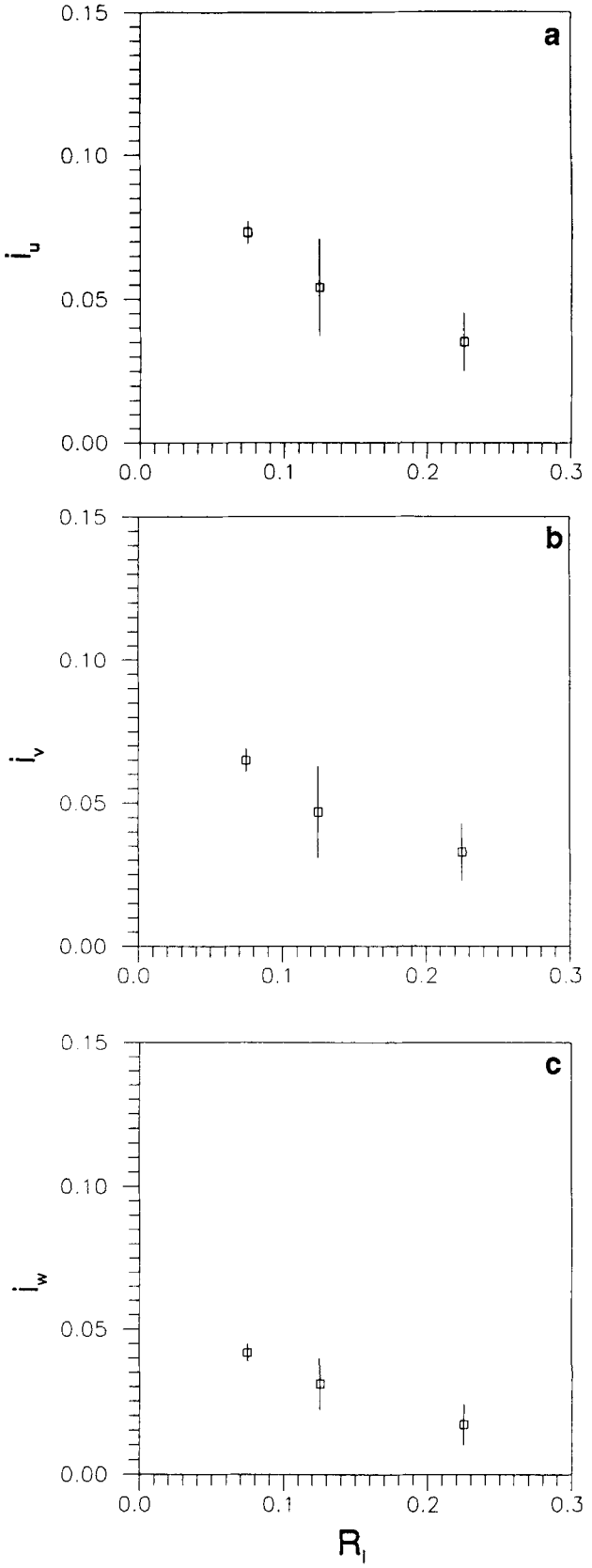


Fig. 17. Turbulence intensities versus Richardson number for **a.** *u* component, **b.** *v* component, **c.** *w* component for 21 June. The bars indicate the standard error.

https://doi.org/10.1017/S0954102095000587 Published online by Cambridge University Press

differences are found with respect to the situation on the previous day (20 June). The eddy transfer coefficients for momentum and heat (Fig. 11a & b) are lower (< 0.40 m s^{-1}) than those obtained the 20 June. These results are related to the increase in stability observed on 21 June, with higher Ri (Fig. 11d) and lower Monin-Obukhov length (Fig. 14); L is <30 m during the whole day at all measured levels. L and K_h are not plotted from 20h00 to 24h00 as counter-gradient fluxes appeared; these situations will be discussed later. Besides, from 20h00 the wind direction changes rapidly with height, so neither Ri nor K_m have been calculated. In these cases it is not physically correct to fit wind profiles, as was discussed in the 'Meteorological data' section. A high correlation is found between K_m, K_h and the friction velocity (Fig. 11c), which may be easily seen comparing their evolutions. Maximum values of K_m and K_h correspond to maximum values of u_*, even though on this day the friction velocity was always <0.2 m s^{-1} . These values show good agreement with the evolution of the turbulent kinetic energy (Fig. 12a). The wind speed at 5m, 17m and 32 m (Fig. 12b) shows a slight decrease during the day, with a big drop from 20h00 onwards at 17 m and 32 m. The main differences with the wind measured on 20 June are: on 21 June, the wind is lower from 0h to 17h at 5m, and a large decrease at 17m and 32 m is seen at the end of the day (20h00–24h00) with $\bar{u} < 5$ m s^{-1}. This lower wind regime allows to have a thermal inversion to persist all day (Fig. 13a).

The thermal behaviour on 21 June is shown in Fig. 13a & b. The inversion is permanent in this day, with $T_{32}-T_2 > 2$°C. There is a strong increase in $T_{32}-T_2$ after 18h00 until 23h00 where $T_{32}-T_2 \simeq 10$°C and a temperature of -29°C at 2 m is reached. The evolution of the sensible heat flux, H, (Fig. 15) can give an explanation of the heating and cooling of the surface temperature (z = 2 m). The increase in temperature takes place when the downward flux has higher values (3h, 8h, 12h and 17h) and the pronounced cooling is produced from 17h00 onwards, when the sensible heat flux approaches zero; then the radiative cooling can not be counteracted by H and the temperature drops quickly, increasing the inversion strength and suppressing the vertical transfer. The evolution of turbulence intensities (i_u, i_v and i_w) for the 21 of June is shown in Fig. 16. They do not present significant variations and only one specific feature will be underlined: there is a local maximum for the three levels at 03h00, concurrent with maxima in K_m, K_h, H, TKE and u_*. This result is typical of a period of internal gravity wave activity, as the Richardson number is high enough to suppress most shear generated turbulence. The different maxima in TKE seen throughout the day seem due to internal wave activity, which includes occasional local breakings.

Nai-Ping *et al.*(1983) and Walter & Overland (1991) have found that counter-gradient fluxes are often associated to gravity-waves, but the counter-gradient fluxes measured here (at 32m (20h00, 22h00) and at 17m (21h00)) are small and they can not be studied. The times of larger eddy transfer, due to internal wave activity, took place at 03h00, 08h00, 12h00 and 17h00 and are matched by higher TKE. A period of low turbulence and no internal wave activity, in spite of the relatively high winds, is present between 13h00 and 16h00 with almost no heat flux.

The relationship between turbulence intensities and Richardson number for the 21 June can be seen in Fig. 17, showing a similar behaviour to that obtained on the previous day although Ri is never less than 0.05 for 21 June and no turbulence intensities can be evaluated in the first interval of Richardson numbers (0–0.05).

Finally, it should be underlined that, from all the results analysed above, the behaviour of the stable boundary-layer is extremely complex and changeable. Sometimes this is not taken into account in the sub-grid parameterizations of the boundary-layer which is required in numerical models. Frequently the turbulent exchanges are quite simplified and K_m and K_h are considered constant, equal, etc. However their values can change rapidly in the stable boundary-layer, and this must be considered in order to improve models.

Conclusions

The main conclusions from the present study of turbulence under stable conditions, which take place during the Antarctic winter are as follows:

a) for Ri approximately >0.1 at 17 and 32 m a strong decrease appeared in the turbulent transfer within the atmospheric boundary-layer, although Ri can be smaller at 5 m. This implies that the upper stability has an important influence on the underlying layers.

b) when the wind shear is high and roughly constant with height the eddy transfer coefficients have also large values, highly dependent on height. In these cases the data show an increase in the eddy transfer coefficients with height.

c) K_m and K_h present very low values (0.01–0.1 $m^2 s^{-1}$) from a certain level of stratification (Ri > 0.15 at 17 and 32 m).

d) the lower atmosphere at Halley is well mixed for wind speeds greater than 10 m s^{-1} at 5 m but as the wind decreases, the vertical turbulent transfer is strongly suppressed near the ground and stable stratification sets in, although winds of speeds > 10 ms^{-1} may occur at the higher levels (17 and 32 m).

e) it has been noted that a decrease in the sensible heat flux produces a drop in the surface temperature, which develops soon after into strong surface thermal inversions. Small counter-gradient fluxes have been sporadically found for high stable stratification. The presence of internal gravity-waves, and then sporadic breaking, is likely to be responsible for these fluxes. The internal wave activity is detected by TKE bursts.

https://doi.org/10.1017/S0954102095000587 Published online by Cambridge University Press

f) turbulence intensities are weakened by stable stratification, and the Richardson number is a useful parameter to characterize the degree of stability under the conditions of the present study.

Acknowledgements

The authors wish to acknowledge the British Antarctic Survey, and especially Dr J. King, for providing the data used in the present study. The comments of Dr S.H. Derbyshire and Dr P.S. Anderson are much appreciated. C.Y. was supported by a MEC scolarship during his visit to United Kingdom.

References

ARYA, S.P.S. 1988. *Introduction to micrometeorology. International Geophysics Series*. London: Academic Press, 307 pp.

BRADLEY, R.S., KEIMIG, F.T. & DIAZ, H.F. 1993. Recent changes in the North American Arctic boundary-layer in winter. *Journal of Geophysical Research*, **98D**, 8851-8858.

BROST, R.A. & WYNGAARD, J.C. 1978. A model study of the stably stratified planetary boundary-layer. *Journal of Atmospheric Sciences*, **35**, 1427-1440.

EGGER, J., WAMSER, C. & KOTTMEIER, C. 1993. Internal atmospheric gravity-waves near the coast of Antarctica. *Boundary-Layer Meteorology*, **66**, 1-17.

EINAUDI F. & FINNIGAN, J.J. 1993. Wave-turbulence dynamics in the stably stratified boundary-layer. *Journal of Atmospheric Sciences*, **50**, 1841-1864.

HALTINER, G.J. & MARTIN, F.L. 1957. *Dynamical and physical meteorology*. New York: McGraw-Hill Book Company, 470 pp.

HUNT, J.C.R., KAIMAL, J.C. & GAYNOR, J.E. 1985. Some observations of turbulence structure in stable layers. *Quarterly Journal of the Royal Meteorological Society*, **111**, 793-815.

KING, J.C. 1990. Some measurements of turbulence over an Antarctic ice shelf. *Quarterly Journal of the Royal Meteorological Society*, **116**, 379-400.

KING, J.C. 1993. Contrasts between the Antarctic stable boundary-layer and the mid-latitude nocturnal boundary-layer. In MOBBS, S.D. & KING, J.C., *eds*. *Waves and turbulence in stably stratified flows*. Oxford: Clarendon Press, 105-120.

KING, J.C. & ANDERSON, P.S. 1988. Installation and performance of the STABLE instrumentation at Halley. *British Antarctic Survey Bulletin*, No. 79, 65-77.

KING, J.C. & ANDERSON, P.S. 1994. Heat and water vapor fluxes and scalar roughness lengths over an Antarctic ice shelf. *Boundary-Layer Meteorology*, **69**, 101-121.

KONDO, J., KANECHICA, O. & YASUDA, N. 1978. Heat and momentum transfers under strong stability in the atmospheric surface layer. *Journal of Atmospheric Sciences*, **35**, 1012-1021.

MOBBS, S.D. & REES, J.M. 1989. Studies of atmospheric internal gravity-waves at Halley Station, Antarctica using radiosondes. *Antarctic Science*, **1**, 64-75.

NAI-PING, L., NEFF, W.D. & KAIMAL, J.C. 1983. Wave and turbulence structure in a disturbed nocturnal inversion. *Boundary-Layer Meteorology*, **26**, 141-155.

NIEUWSTADT, F.T.M. 1984. The turbulent structure of the stable nocturnal boundary-layer. *Journal of Atmospheric Sciences*, **41**, 2202-2216.

PASRICHA, P.K., SINGH, R, SARKAR, S.K., DUTTA, H.N., REDDY, B.M. & DAS, P.K. 1991. Characteristics of atmospheric turbulence in the surface layer over Antarctica. *Boundary-Layer Meteorology*, **57**, 207-217.

REES, J.M. 1987. The propagation of internal gravity-waves in the stably stratified atmospheric boundary-layer. *Annales Geophysicae*, **5B**, 421-432.

REES, J.M. 1991. On the characteristics of eddies in the stable atmospheric boundary-layer. *Boundary-Layer Meteorology*, **55**, 325-343.

REES, J.M. & MOBBS, S.D. 1988. Studies of internal gravity-waves at Halley Base, Antarctica. *Quarterly Journal of the Royal Meteorological Society*, **114**, 939-966.

SMEDMAN, A.S. 1991. Some turbulence characteristics in stable atmospheric boundary-layer flow. *Journal of Atmospheric Sciences*, **48**, 856-868.

STULL, R.B. 1988. *An introduction to boundary-layer meteorology*. Dordrecht: Kluwer Academic Publishers, 666 pp.

WALTER, B. & OVERLAND, J.E. 1991. Aircraft observations of the mean and turbulent structure of the atmospheric boundary-layer during spring in the Central Arctic. *Journal of Geophysical Research*, **96C**, 4663-4673.

WITTICH, K.P. & ROTH, R. 1984. A case study of nocturnal wind and temperature profiles over the inmohogeneous terrain of Northern Germany with some considerations of turbulent fluxes. *Boundary-Layer Meteorology*, **28**, 169-193.

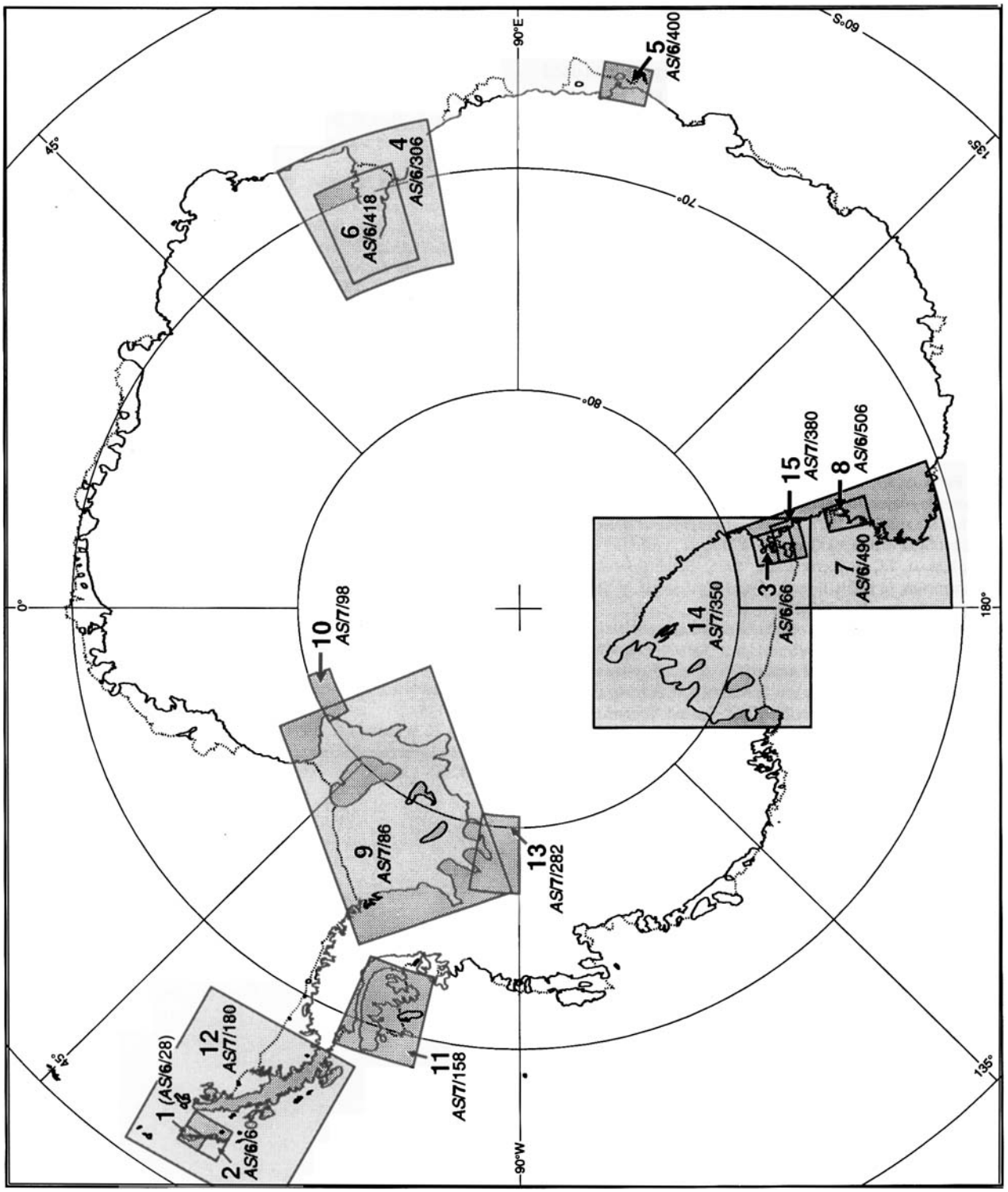
WYNGAARD, J.C. 1973. On Surface Layer turbulence. *In* HAUGEN, D.A., *ed.* Workshop on Micrometeorology. *American Meteorological Society*, 101-148.

YAGÜE, C. & CANO, J.L. 1994. The influence of stratification on heat and momentum turbulent transfer in Antarctica. *Boundary-Layer Meteorology*, **69**, 123-136.

https://doi.org/10.1017/S0954102095000587 Published online by Cambridge University Press

Antarctic Science **Handy Atlas Map No. 16.**

This map provides an index to the Handy Atlas Map Series prepared so far for *Antarctic Science* by Sarah King, at the British Antarctic Survey. This series of maps have been generated from the SCAR Antarctic Digital Database, and customized by the addition of place names. Publication references to the maps are given thus: AS/**6**/28 = *Antarctic Science*/**6**/p.28.



https://doi.org/10.1017/S0954102095000587 Published online by Cambridge University Press